
# Strathprints Institutional Repository

# Design and Trade-offs of a Pole-Sitter Mission

Matteo Ceriotti,* Jeannette Heiligers† and Colin R. McInnes‡
*University of Strathclyde, Glasgow G4 0LT, United Kingdom*

**This paper provides a mission analysis and systems design of a pole-sitter mission, i.e. a spacecraft that is continuously above an Earth Pole, and can provide real-time, continuous and hemispherical coverage of the polar regions. Two different propulsion strategies are proposed: solar electric propulsion (SEP) and SEP hybridized with a solar sail. For both, minimum-propellant pole-sitter orbits and transfers are designed, assuming Soyuz and Ariane 5 launch options. A mass budget analysis allows for a trade-off between mission lifetime and payload mass capacity (up to 7 years for 100 kg), and candidate payloads for a range of applications are investigated.**

## I. Introduction

SPACECRAFT in geostationary orbit (GEO) have demonstrated the significant benefits offered by continuous coverage of a particular region. However, GEO platforms can only provide their services in the equatorial and temperate zones, where elevation angles are sufficiently high. At higher latitudes, similar services are provided at present by mainly two types of conventional platforms: highly-eccentric, inclined orbits, or low or medium polar orbits.

The first class includes the well-known Molniya-type orbits: they exploit the oblateness of the Earth (effect of the $J_2$ term in the geopotential) to maintain the argument of the pericentre constant in time [1]. In order to achieve this condition, their inclination must be fixed at the critical value of 63.4°. This value is still relatively low to obtain a satisfactory coverage not only of the polar caps, but also of the high-latitude regions [2]. Due to their high eccentricity, the orbit apocentre is usually at a distance that is comparable to GEO, and therefore offers a hemispheric view of the Earth. However, an intrinsic limitation is the impossibility of providing continuous coverage over time: despite that the spacecraft spends a significant fraction of its orbital period around the orbit apocentre, the viewing conditions of the poles change continuously, and there is an interval of time in which the

* Currently Lecturer at School of Engineering, James Watt Building South, University of Glasgow, Glasgow G12 8QQ, United Kingdom. Tel: +44 141 330 6465. Email: matteo.ceriotti@glasgow.ac.uk
† Research Associate, Advanced Space Concepts Laboratory, Department of Mechanical and Aerospace Engineering, 141 St. James Road. Tel: +44 141 548 5989. Email: jeannette.heiligers@strath.ac.uk
‡ Director, Advanced Space Concepts Laboratory, Department of Mechanical and Aerospace Engineering, 141 St. James Road. Tel: +44 141 548 2049. Email: colin.mcinnes@strath.ac.uk

spacecraft is at the pericentre and coverage is not available. With an orbital period of approximately 12 hours, it has been shown that three to six Molniya spacecraft are necessary to provide satisfactory continuous coverage [3]. Recent research [4] has considered changing the critical inclination of the Molniya orbit to 90°, using a continuous acceleration generated by a solar electric propulsion (SEP) system for maintaining the orbit. However, a continuous and constant polar view is not available.

The second class of orbits largely consists of Sun-Synchronous orbits. Spacecraft in these orbits are used due to the high spatial resolution that they can provide. However, only a narrow swath is imaged at each polar passage, relying on multiple passages (and/or multiple spacecraft) for full coverage. For example, Landsat 7 (altitude of 705 km at 98.2°) completes just over 14 orbits per day, covering the entire Earth between 81 degrees north and south latitude every 16 days.[*] This results in a poor temporal resolution for the entire polar region, as different areas are imaged at different times, hence missing the opportunity to have a simultaneous and continuous real-time view of the pole. At present, these images are post-processed to make a composite image, which can be used, for example, for weather forecasting and wind vector prediction. However, the data that can be extracted is neither complete nor accurate [5].

To overcome these limitations, the ideal platform would be one constantly above one of the poles, stationary with respect to the Earth, in the same way as a GEO spacecraft is stationary above one point on the equator. In this position, the footprint of the spacecraft will be constantly at the pole, in the same way as the footprint of a geostationary spacecraft is constantly at some longitude on the equator. This spacecraft is known in literature as "pole-sitter", which uses low-thrust propulsion to maintain a position along the polar axis (see Fig. 1). The pole-sitter is the only platform that can offer a truly continuous hemispheric view of one of the poles, enabling real-time imaging over the entire disc (Fig. 1b). The first study of this concept was apparently made by Driver [6] in 1980.

[*] Landsat 7 Handbook, http://landsathandbook.gsfc.nasa.gov/ [Cited 17/08/2012]

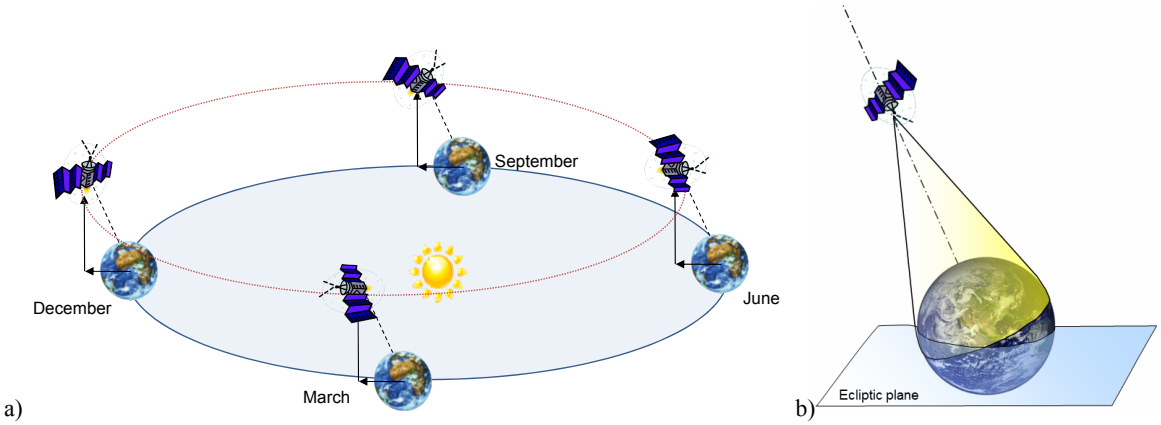


**Fig. 1 Pole-sitter concept in (a) Sun-centered inertial frame and (b) Earth-centered frame.**

Driver proposed the use of solar electric propulsion (SEP) to maintain the pole-sitter position counterbalancing the gravitational forces. Despite the high efficiency of SEP, the thrusting time and hence the mission duration is always limited by the mass of propellant on-board.

In order to avoid this drawback, some authors investigated the use of a solar sail [7] instead of SEP as a means to provide the continuous acceleration. Solar sailing is a propellant-less spacecraft propulsion system that exploits the solar radiation pressure due to solar photons impinging on a large, highly reflecting surface (the sail) to generate thrust. Solar sails have been recently demonstrated in space [8, 9] and due to the interesting potential of providing acceleration without propellant mass, they seem to be suitable for potentially long duration missions that require a small, but continuous, thrust, such as the pole-sitter. One of the intrinsic limitations of solar sailing is the relationship between the direction of the sail force vector and its magnitude; in particular, the force can never be directed towards the Sun, which is the reason why a sailcraft cannot maintain the pole-sitter position indefinitely [10]. Other stationary positions in the Sun-Earth system [11] and non-Keplerian orbits [12] were studied in the literature, however the spacecraft does not achieve satisfactory conditions for continuous coverage of high-latitude regions.

In order to overcome the limitations of a platform based on a pure sail, which constrains the positions (or more generally the orbits) that can be achieved and maintained, hybrid propulsion has been proposed [13]. Hybridizing SEP and solar sailing is a comparatively recent idea [13], nevertheless research is flourishing in this field, investigating its potential for novel, interesting applications [14-18]. The reason for this interest is due to the fact that in the hybrid system, at the cost of increased spacecraft and mission design complexity, the two propulsion systems complement each other, cancelling their reciprocal disadvantages and limitations. While the hybrid propulsion pole-sitter can in principle enable a mission that is not feasible using only a solar sail and can extend the mission lifetime with respect to the pure SEP scenario, there are still issues associated with the pole-

sitter mission related to the large distance from the Earth. As expected, the acceleration required increases dramatically as the spacecraft is stationed closer to the Earth, and reasonable values of acceleration are obtained only if the Earth-spacecraft distance is of the order of millions of kilometers [6, 10]. Nevertheless, the advantage of having a static or quasi-static platform is such that these concepts are worth considering and investigating in more detailed studies [19]. Although high-bandwidth telecommunications and high-resolution imagery are difficult due to the large Earth-spacecraft distance, a number of novel potential applications are enabled, both in the fields of observation and telecommunications, which will be discussed in the paper. Due to these capabilities, and with the aim of increasing mission lifetime, the authors have undertaken an extensive investigation focused on the concept of a hybrid-propulsion pole-sitter: from the generation of optimal hybrid pole-sitter orbits [10], to system mass budgets [20], and from design of optimal transfers to the pole-sitter orbit from LEO [21], to design of optimal north-to-south transfers [22].

This paper presents the full mission and systems analysis of a pole-sitter mission, covering the launch phase and the operational phase. Several different options will be proposed and assessed, including different propulsion systems for the spacecraft (SEP or hybrid sail-SEP), different mission scenarios, enabling coverage of one pole only or both poles, and different launcher options. Then a systems design will determine the lifetime of the spacecraft, and some candidate payloads will be identified to enable the potential applications of the pole-sitter.

## II. Mission Description and Propulsion Options

### A. Mission Phases

The complete pole-sitter mission is split into different phases, which will be described in detail and designed in the following sections. The phases are schematically represented in Fig. 2.

The mission starts with a launch and transfer phase. This phase begins with the spacecraft injected into a low Earth orbit (LEO) by the launcher; the type and size of the LEO depends on the launcher used. The launcher upper stage provides a number of impulsive maneuvers, before jettisoned; the spacecraft continues the transfer using its own low-thrust propulsion system, up to the injection point into the pole-sitter orbit.

At this point, the operational phase begins. The operational phase is the one in which the spacecraft is stationed along the polar axis of the Earth, maintaining its nominal pole-sitter orbit. This is obviously the most important phase of the mission, and its duration shall be maximized.

Since each pole is lit only 6 months per year, it is an option, especially for observations in the visible part of the spectrum, to transfer the spacecraft from a North Pole operational orbit to a symmetric orbit below the South Pole, and vice-versa, according to their lighting conditions. Therefore, an additional north-to-south transfer phase

is designed. This phase can be inserted at appropriate points along the nominal orbit to enable the transfer to the other pole, where a symmetric operational orbit can be followed.

These three phases will be described and designed sequentially, starting from the operational phase, which defines the optimal nominal orbit. Then, the transfer from Earth to this orbit will be designed. The optimization of the transfer allows the determination of the maximum mass at the pole-sitter orbit injection, and therefore the spacecraft can be sized and the lifetime assessed. Finally, the north-to-south transfers will be designed, between optimal pole-sitter orbits.

The design of the three phases requires the solution of optimal control problems, which are solved numerically using a direct method based on pseudospectral transcription, implemented in the tool PSOPT [23], and the non-linear programming problem is solved through IPOPT (interior point optimizer, [24]).

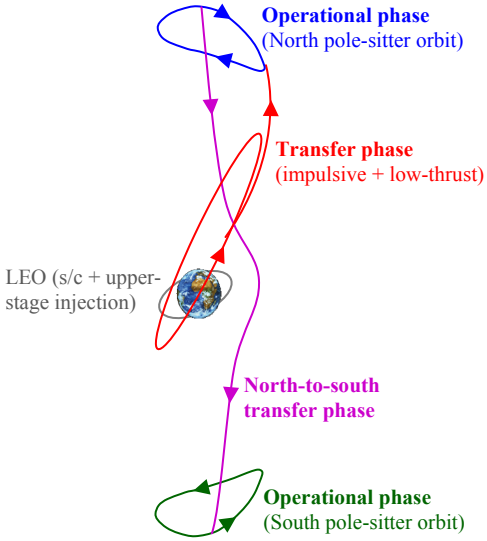


**Fig. 2 Representation of the mission phases.**

*1. Trajectory models*

For the transfer and operational phases we consider a three-body problem in which the spacecraft is subject to the gravitational attraction of both the Earth and the Sun. This choice is made since the gravity of the Earth and the Sun are both important for a practical pole-sitter. In particular, we use the well-known circular restricted three-body problem (CR3BP), which describes the motion of the spacecraft, of negligible mass, under the influence of the Sun and Earth (the *primaries*) that rotate in circular motion around each other (at a constant distance of 1 Astronomical Unit, AU). The reference frame is synodic, with its origin at the center-of-mass of the system, the x-axis passing through the Sun and the Earth, and oriented towards the latter, and the z-axis

perpendicular to the ecliptic plane, see Fig. 3. The equations of motion for the spacecraft can be found in Ref. [10].

Note that the launch phase, which occurs close to the Earth, will be modeled using a two-body approach. Details of this model will be given in Section III.B.

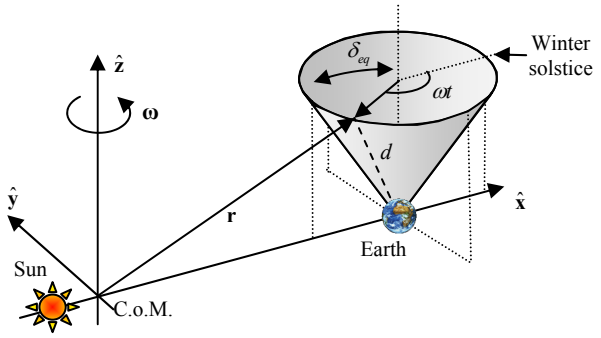


**Fig. 3 Synodic reference frame of the restricted three-body problem and pole-sitter reference.**

## B. Spacecraft Propulsion Options

We consider two different spacecraft architectures. The first is a pure SEP spacecraft, in which solar electric propulsion is used to provide the acceleration required throughout the mission. The spacecraft complexity is relatively low in this case, due to the high TRL of this type of propulsion system. The second is a more advanced, long-term spacecraft that exploits both solar sail and solar electric propulsion on the same bus.

### *1. Pure SEP*

The pure SEP spacecraft can be considered as a conventional spacecraft with deployable solar arrays to power the propulsion system. Usually, the solar panels can be rotated along their longitudinal axis, so as to modulate the power delivered according to the instantaneous need of the spacecraft. The thruster is assumed to be rigidly connected to the spacecraft bus, and the thrust vector is steered by changing the attitude of the spacecraft (the instruments can be mounted on a gimbal).

The key technology parameters of an SEP thruster are the maximum thrust that it can provide, usually in the order of a fraction of a Newton, and its specific impulse. In this paper, we assume that the maximum thrust is used to size the SEP system, as will be explained later, and a fixed specific impulse of 3200 s is conservatively assumed, based on current ion engine technology (existing NSTAR/DS1 [25] or EADS/Astrium RIT-XT [26]). It is foreseen that this specific impulse allows levels of thrust suitable for the spacecraft and mission under consideration.

Since the fuel mass consumption is directly related to the magnitude of the thrust, in general we will try to find trajectories that minimize propellant consumption, in order to maximize the mission lifetime, or alternatively, to maximize the payload mass for a given lifetime.

## 2. *Hybrid Sail and SEP*

In this scenario, we envisage the use of a spacecraft that combines solar sailing and SEP. As noted earlier, this adds system complexity, but it can be advantageous in terms of mission lifetime, as it will be shown in this paper.

The hybrid spacecraft has a bus from which the sail is deployed, and thus the sail is rigidly connected to it (see Fig. 4). We assume that the sail can be steered, with relatively modest angular acceleration, by using the attitude control system of the spacecraft. The SEP thruster is mounted on a gimbal system, because it is required that the SEP thrust vector can steer independently of the sail orientation, for control purposes. Furthermore, the SEP system requires electrical power in order to operate. In conventional spacecraft, this is collected through solar arrays that are hinged on the spacecraft bus and can be oriented towards the Sun when power is needed. This type of architecture would be difficult to implement due to the presence of the sail. We instead envisage a layer of thin film solar cells (TFSC) which partly occupy the sail surface, similarly to the IKAROS spacecraft [27].

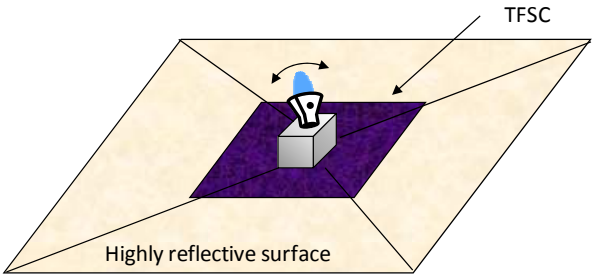


**Fig. 4 Hybrid spacecraft with sail, thin film solar cells and steerable thruster.**

We assume a partially reflective, partially absorbing solar sail (optical sail model) of total area $A_s$, such that the solar radiation pressure generates an acceleration with a component perpendicular to the sail and one parallel to it [13, 14]. The sail acceleration is proportional to the parameter $\beta$, the *system lightness number*, which is a function of the sail loading $\sigma = m/A$ of the spacecraft (spacecraft mass over total sail area):

$$\beta = \sigma^* / \sigma \tag{1}$$

with $\sigma^* \cong 1.53 \cdot 10^{-3}$ kg/m$^2$ the critical sail loading. However, $\beta$ can also be defined as the ratio of the maximum solar radiation pressure acceleration at 1 A.U. (*sail characteristic acceleration*) to the gravitational acceleration. Note that $\beta$ varies during the mission, because of the decrease in spacecraft mass *m* due to SEP propellant consumption. We therefore introduce the value $\beta_0 = \beta \frac{m}{m_0}$, constant, in which the subscript "0" refers to the parameters at the injection into the pole-sitter operational orbit, when the time is $t_0$. Note that the pure SEP spacecraft can be considered as a particular hybrid system with $\beta = \beta_0 = 0$. Values of $\beta$ up to 0.05 can be assumed for a near-term hybrid system [28]. Recent solar sail demonstrators, however, had considerably lower lightness numbers: JAXA's IKAROS [29] has a 20-m-diagonal square sail and weighs 350 kg ($\beta$ = 0.001), while NASA's NanoSail-D2 [9] is 4 kg for 10 m$^2$ ($\beta$ = 0.003).

In the hybrid spacecraft, the TFSCs are assumed to cover an area $A_{TF} = 0.05A$ on the sail. This area ratio is a conservative estimation based on previous studies [14] and the IKAROS mission [29], and it is used to compute the optimal orbits. The actual value of this area depends on the spacecraft technology parameters, as well as the selected orbit, and will be computed in Section IV.

Another important technological parameter of a sailcraft is the areal density of the sail assembly, $\sigma_s$. It measures the mass of the sail per unit surface area, and it is expected that technological developments [28] should enable sails of 10 g/m$^2$ in the near future. Ultra-thin (around 2 μm of thickness) sails are expected in the mid- to far-term timeframe [30] and can lead, for large sails, to sail loadings of the order of 5 g/m$^2$.

Given these considerations, the value of $\beta_0$ for the hybrid scenario can be decided following the study in Ref. [20]. That work showed that, if a sail assembly areal density of 10 g/m$^2$ is considered, then the hybrid spacecraft is beneficial only if very long missions are considered (i.e. lifetime > 7 years). Instead, considerable mass saving (or extended lifetime) is expected considering a hybrid system with $\sigma_s = 5$ g/m$^2$ (or below). Furthermore, for this value, it is found that that $\beta_0 = 0.035$ represents the lightness number in which the spacecraft initial mass, for a given payload, is lowest over a range of mission lifetimes. For these reasons, we select for this scenario: $\beta_0 = 0.035$, $\sigma_s = 5$ g/m$^2$.

## III. Mission Design

### A. Pole-Sitter Operational Orbits

An optimal pole-sitter orbit is defined as the one that minimizes the propellant consumption of the spacecraft, while maintaining the pole-sitter condition at any time, and being one-year periodic. The design of this orbit

requires the (numerical) solution of a constrained optimal control problem, in which the control and state history over time is to be determined. Details of the optimization process are presented in Ref. [10].

In the optimization process, the distance from the Earth can vary, however a maximum is set to $d_{max} = 0.01831\,\text{AU}$, i.e. 2.74 million km, in order to prevent the trajectory from going too far away from the Earth, thereby excessively decreasing the spatial resolution for instruments or the data bandwidth of the platform. In fact, it was found [10] that optimal, unconstrained trajectories move further away from the Earth in summer, which is the period in which the North Pole is lit, and therefore observations at optical wavelengths can be performed.

The result of the optimization, for the two scenarios, is presented in the following figures. Note that the figures showing the orbits (or later on in the paper, the transfers) employ a Sun-Earth synodic reference frame centered at the Earth rather than at the Sun-Earth barycenter for interpretation purposes. The optimal SEP-only path is essentially symmetric around spring and autumn, and the spacecraft is closest to the Earth at the summer and winter solstices. Instead, in the hybrid case, the spacecraft is closest to the Earth in winter and farthest in summer: the constraint on the maximum distance is active across the summer solstice for approximately 150 days. This can be seen in Fig. 5. The same figure also highlights that the SEP spacecraft distance to Earth varies between 0.01568 and 0.01831 AU, while for the hybrid case it varies between 0.01369 and 0.01831 AU.

It results also that the SEP acceleration required is less for the hybrid spacecraft than for the pure SEP spacecraft. This is expected, as the sail provides a beneficial contribution to the total acceleration, and results in propellant mass saving. For example, for a spacecraft of mass 1000 kg at injection, the maximum SEP thrust would be 170 mN for the pure SEP system, and 144 mN for the hybrid system. At this point, however, the spacecraft mass is still unknown: it will be determined by the launcher capability and the transfer phase.

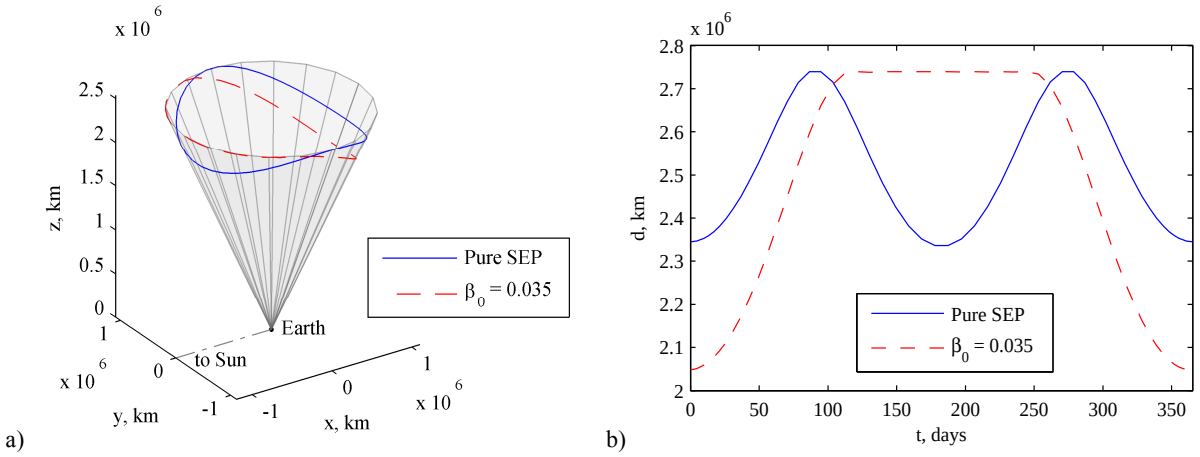


**Fig. 5 Fuel-optimal pole-sitter orbits for the pure SEP case and the hybrid case. (a) Optimal trajectories in the synodic reference frame. (b) Distance from the Earth.**

## B. Launch and Transfer Phase

In order to find the maximum mass that can be inserted into the pole-sitter orbit, this section investigates optimum transfers from LEO up to insertion into the pole-sitter orbit. The transfer is modeled as a launch phase and a transfer phase, as shown in Fig. 2. The launch phase is designed as an impulsive, two-body Soyuz or Ariane 5 upper-stage transfer from a low Earth parking orbit up to insertion into the transfer phase. The transfer phase is modeled in the Earth-Sun three body problem using either pure SEP or hybrid propulsion, depending on the system architecture. The overall objective is to maximize the mass upon insertion into the pole-sitter orbit, assuming that the full launch vehicle capacity into the parking orbit is used. More details on this approach can be found in Ref. [21] . Table 1 provides data of the Soyuz and Ariane 5 parking orbits, as well as performances in terms of mass deliverable to these parking orbits and characteristics of their upper stages.

**Table 1 Soyuz and Ariane 5 parking orbit and launch vehicle specifications**

| Launcher | Parking orbit | | | Upper stage | | Adapter |
|---|---|---|---|---|---|---|
| | Altitude, km | Inclination, deg | Performance, kg | Mass, kg | Specific impulse, s | Mass, kg |
| Soyuz | 200 | 51.8 | 7185 | 1000 | 330 | 100 |
| Ariane 5 | 400 | 51.6 | 19000 | 4540 | 446 | 160 |

The resulting optimal transfers, see Fig. 6a, inject the spacecraft into the operational orbit at winter solstice, i.e. at the point closest to the Earth. More details on the optimal transfers, including the maximum thrust magnitude and mass injected into the pole-sitter orbit can be found in Table 2.

Since the SEP and hybrid pole-sitter orbits are not the same, a direct comparison of the performances of the transfers using the two propulsion techniques cannot be made. However, the mass injected into the hybrid pole-sitter orbit is larger than for the SEP case: an increase of 58 kg for a Soyuz launch and an additional 160 kg for an Ariane 5 launch. Part of this better performance will be due to the smaller Earth to pole-sitter distance at

winter solstice (i.e. upon injection) for the hybrid pole-sitter orbit. However, part will also be due to the smaller propellant consumption in the transfer, because the hybrid case allows for a much longer duration in which the SEP thruster is switched off due to the contribution of the solar sail, see Fig. 6b. However, the total transfer duration is considerably longer.

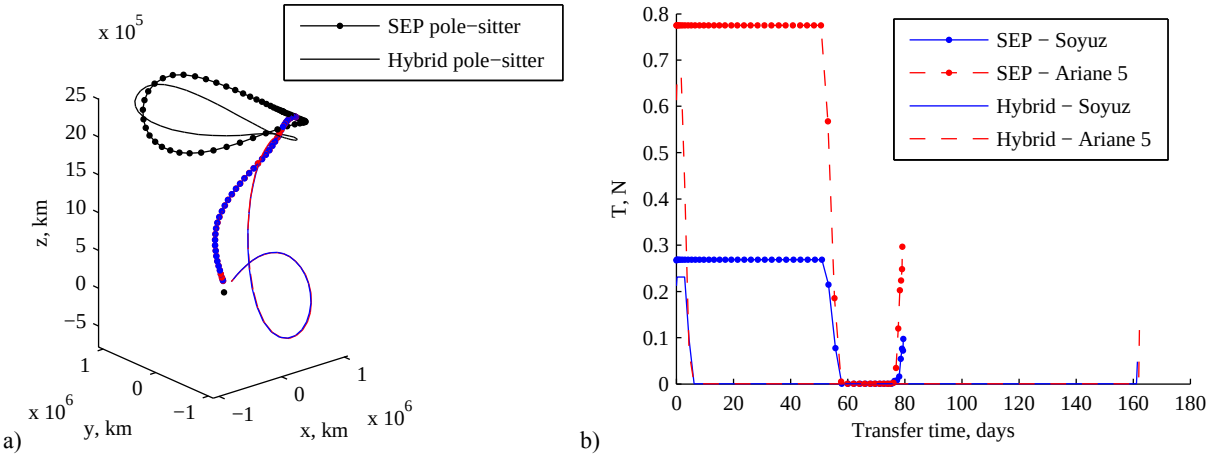


**Fig. 6 Optimal transfers for SEP and hybrid propulsion with Soyuz and Ariane 5 launches. (a) Transfer in synodic reference frame. (b) Thrust profile.**

**Table 2 Results for the optimization of transfer to SEP and hybrid low-thrust pole-sitter orbits including the maximum SEP thrust magnitude and the mass injected into the pole-sitter orbits.**

| Architecture | Launcher | Transfer time, d | $T_{max}$ , N | $m_0$ , kg |
|---|---|---|---|---|
| SEP | Soyuz | 79 | 0.269 | 1537 |
| SEP | Ariane 5 | 79 | 0.775 | 4439 |
| Hybrid | Soyuz | 161 | 0.231 | 1595 |
| Hybrid | Ariane 5 | 161 | 0.667 | 4599 |

### C. Transfers between North and South Poles

Due to the tilt of the Earth's polar axis with respect to the ecliptic plane, the North and South Poles are alternately situated in darkness for 6 months per year. For observations being performed in the visible part of the spectrum, this significantly constrains the mission scientific return. Therefore, an additional transfer is introduced that allows the pole-sitter spacecraft to change between pole-sitter orbits above the North and South Poles before the start of the Arctic and Antarctic winters, see Fig. 2. For that, the SEP and hybrid pole-sitter orbits shown in Fig. 5 are mirrored in the ecliptic plane. Viewed in the synodic frame, the Poles are illuminated when the spacecraft is in the Sun-ward part of the pole-sitter orbit, see Fig. 7. Ideally, this means that the pole-sitter spacecraft would follow the north pole-sitter orbit from March to September and the south pole-sitter orbit from September to March. Clearly, in reality this is not feasible since some time needs to be allowed for the

spacecraft to transfer from north to south and vice-versa. Instead, departure takes place between summer and autumn (June – September), while arrival takes place between autumn and winter (September – December), see Fig. 7, where this paper conventionally refers to the seasons in the northern hemisphere. Note that due to the symmetry of the problem, the optimal transfers from north to south can also be used to transfer from south to north.

The concept of transfers between north and south pole-sitter orbits has been introduced before [22], and is applied in this section to the optimal SEP and hybrid pole-sitter orbits of Fig. 5 (using the respective types of propulsion to perform the transfer). Also, for both propulsion strategies, both the Soyuz and Ariane 5 launch cases will be considered together with the corresponding values for the maximum thrust magnitude as provided in Table 2.

In the transfer design, a tradeoff has to be made between the observation time on the operational orbit (which shall be maximized), and the propellant consumption required for the transfer: a fast transfer guarantees long observation times, but requires more propellant.

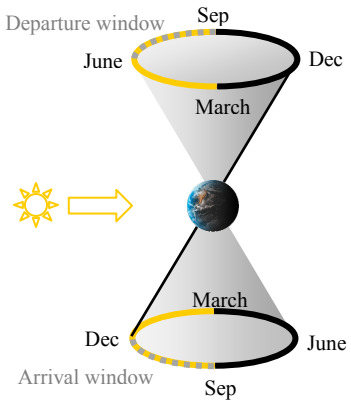


**Fig. 7 Schematic of dark (black line) and light (yellow line) conditions on the North and South Poles during the year and departure and arrival window (dotted) for a north-to-south transfer.**

For the pure SEP spacecraft, a transfer that guarantees about 90 days of observation time in the operational orbit per year for each Pole uses as much propellant as the operational orbit itself. If the minimum-propellant (i.e. longest) transfer is used, the observation time reduces to 54 days, however the gain in propellant mass is 279.6 kg after 5 years, with respect to staying on the same pole-sitter orbit. On the other end, observation times of up to 94 days can be achieved, by using the quickest transfer. This comes, however, at the cost of an increase in the propellant consumption (45.3 kg more are required over 5 years). Very similar results are obtained for the hybrid case. Note that in the following, the minimum-propellant transfers are used.

### D. Full Mission Profile

Finally, to illustrate the full mission profile, Fig. 8 and Fig. 9 represent the trajectory of the pole-sitter spacecraft, including the launch phase, operational phases and north-to-south transfers. Fig. 8 refers to the pure SEP mission, Fig. 9 to the hybrid propulsion one. Both figures represent the Ariane 5 option; the trajectory followed by the Soyuz option is very similar. In each figure, the plot (a) is in an Earth-centered synodic reference frame (Earth and Lagrange points $L_1$ and $L_2$ are represented with dots), while the plot (b) is in an inertial, Sun-centered reference frame (the Sun represented with a dot, and the orbit of the Earth with a solid black line). Note that in plots (b) the z-direction is not to scale with x and y, in order to appreciate the out-of-plane displacement of the pole-sitter, which would otherwise be too small with respect to the orbit of the Earth.

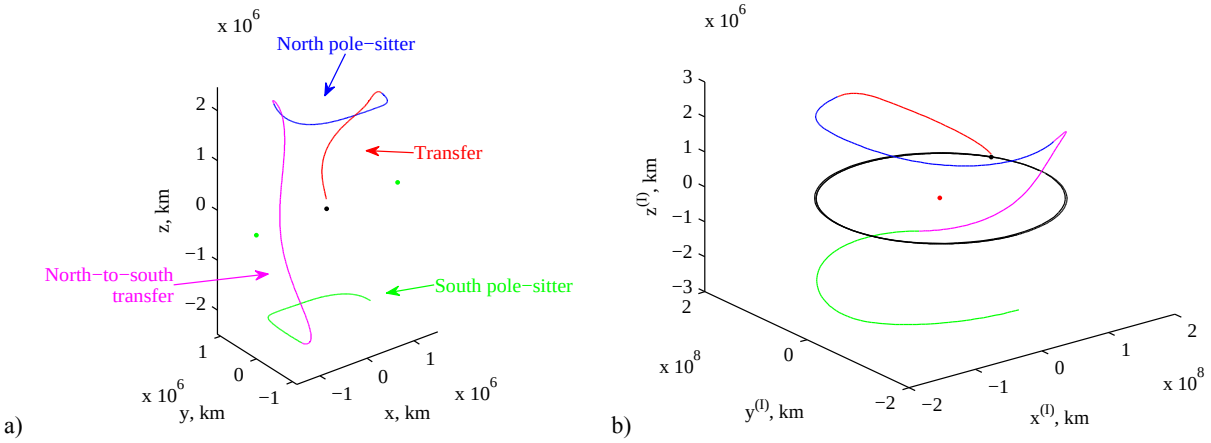


**Fig. 8 Pure SEP mission trajectory (Ariane 5 launch) in synodic reference frame (a) and inertial Sun-centered reference frame (b).**

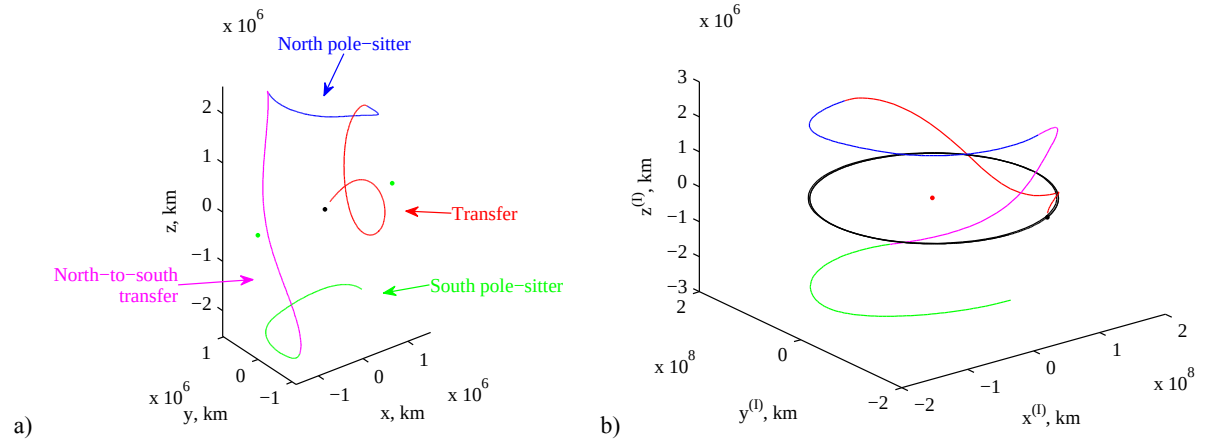


**Fig. 9 Hybrid propulsion mission trajectory (Ariane 5 launch) in synodic reference frame (a) and inertial Sun-centered reference frame (b).**

## IV. Spacecraft Subsystems Sizing

Starting from the total mass $m_0$ that can be injected into the operational orbit of the pole-sitter (Table 2), a systems design provides the mission lifetime that can be achieved into this orbit, or alternatively the payload mass that can be carried for a given lifetime of the spacecraft. For a preliminary mass budget, the total mass of the pure SEP spacecraft can be split into propellant, tank, SEP thruster, solar arrays, other subsystems and payload. For the hybrid spacecraft, instead, we also consider the gimbal of the SEP thruster, the sail, and the radiators to dissipate any excess of power collected by the sail-mounted thin film solar cells.

Note that the systems mass budget proposed here differs to the one in Ref. [20] in several ways: it considers multiple SEP thrusters, but working in parallel to achieve the necessary thrust, rather than being redundant; the mass of the other subsystems (ADCS, thermal, structure, OBDH, TT&C) is taken into account explicitly, as 30% [1] of the spacecraft dry mass; the pure SEP spacecraft does not employ thin film solar cells, but solar arrays mounted on panels (higher efficiency and areal mass); the pure SEP spacecraft does not employ a gimbal system, as it is assumed that attitude maneuvers can be used to steer the thrust vector; lastly, margins are also taken into account for each subsystem [1]. In particular, the sail and the thin film solar cells are considered new technologies, and therefore a margin of 20% is used. Conversely, the other subsystems are considered to be well-proven technologies, and its margin is set to 5%. The same margin is added to the propellant mass for contingency maneuvers.

Given the initial mass of the spacecraft in the pole-sitter orbit (as found in Table 2 for a given mission scenario), the optimal 1-year trajectory is used to compute the propellant mass $m_{prop}$ needed for a given lifetime $t_{mission}$. Once the propellant mass is found, the mass budget returns the payload mass $m_{pl}$. This is plotted, as a function of the lifetime, in Fig. 10. Each plot refers to one spacecraft architecture (pure SEP, hybrid).

It can be noted that the mission lifetime does not depend on the injected total mass $m_0$, but only on the technology that is used to build the spacecraft. The lifetime for the pure SEP system is limited to approximately 4.5 years, while this value extends to about 7 years for the hybrid architecture. This result itself should be sufficient to justify the interest in the hybrid propulsion technology for this type of mission, and in general for all those missions which require a continuous acceleration [20]. Furthermore, for nearly equal injected masses, the hybrid spacecraft can carry the same payload mass for a longer mission lifetime. Finally, for a particular spacecraft architecture, the payload mass scales with the injection mass $m_0$.

Considering a 100-kg payload mass, launching with Soyuz, the lifetime is 3.6 years if the spacecraft is using pure SEP technology, or 5.6 years if using hybrid propulsion. These lifetimes extend to 4.24 and 6.58 years when launching with Ariane 5 for the two architectures respectively.

The subsystem design also allows the computation of the mass of the other subsystems, some of which are reported in Table 3. The size of the total sail assembly (reflective surface and thin film solar cells) of the hybrid spacecraft is 191 m for the Soyuz launch and 324 m for the Ariane launch, assuming a square assembly.

The hybrid configuration furthermore allows a lower power budget, by reducing the thrust needed per unit mass of the spacecraft from the SEP thruster. For the pure SEP spacecraft, the maximum power required by the SEP thruster is 6 kW (Soyuz) and 17.4 kW (Ariane 5). For the hybrid spacecraft, instead, the power is 5.2 kW (Soyuz) and 15 kW (Ariane 5), despite the fact that the total injected mass of the spacecraft, $m_0$, is slightly larger than in the SEP case.

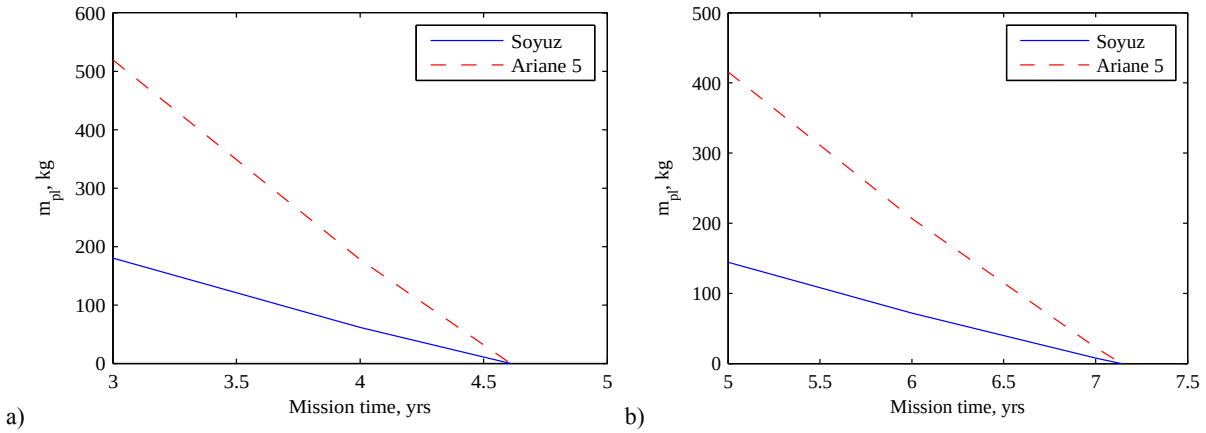


**Fig. 10 Payload mass ($m_{pl}$) as a function of the mission lifetime, for the pure SEP spacecraft (a) and the hybrid spacecraft (b).**

**Table 3 Design points. Masses are without margins.**

| Architecture | Pure SEP | | Hybrid | |
|---|---|---|---|---|
| Launcher | Soyuz | Ariane 5 | Soyuz | Ariane 5 |
| Lifetime, $t_{mission}$, yrs | 3.6 | 4.24 | 5.6 | 6.58 |
| Payload mass, $m_{pl}$, kg | 100 | 100 | 100 | 100 |
| Pole-sitter injection mass, $m_0$, kg | 1537 | 4439 | 1595 | 4599 |
| SEP mass, kg | 121 | 348 | 104 | 299 |
| Propellant mass, $m_{prop}$, kg | 675 | 2192 | 698 | 2242 |
| Other subsystems mass, kg | 259 | 674 | 269 | 707 |
| Solar array/TFSC area, $m^2$ | 44 | 127 | 121 | 349 |
| Solar sail mass (reflective), kg | - | - | 182 | 524 |
| Total sail area (reflective + TFSC), $m^2$ | - | - | 191 × 191 | 324 × 324 |
| Maximum SEP thrust, mN | 269 | 776 | 231 | 667 |
| Maximum SEP power, kW | 6 | 17.4 | 5.2 | 15.0 |

### A. Payload Selection and Applications

We now wish to investigate possible payloads that could be used on the pole-sitter spacecraft. As noted in the introduction, the pole-sitter spacecraft could serve as a platform for Earth observation and science, and a data relay for telecommunications. Concerning the former, taking into account the considerable distance of the spacecraft from the Earth, high-resolution imaging is limited to the near-visible part of the spectrum (from infrared to ultra-violet). Spatial resolution in the visible wavelength in the range 10-40 km should be available for the pole-sitter [1], which enables real-time, continuous views of dynamic phenomena and large-scale polar weather systems [19]. The creation of atmospheric motion vectors (AMV) would also make use of the stationary location of the platform, avoiding gap problems related to geolocation and intercalibration that composite images introduce [5]. Glaciology and ice-pack monitoring would also benefit from continuous, but low resolution polar observation [5]. Ultraviolet imagery of the polar night regions at 100 km resolution or better would enable real-time monitoring of rapidly-changing hot spots in the aurora that can affect high frequency communications and radar [19]. As the resolution degrades with increasing wavelength, it is unlikely that sensing in the microwave band could provide some useful information. However, radio science can detect the total flux of radiation reflected and emitted by the Earth at the poles.

Candidate instruments are found in the literature of deep space missions. In fact, optics for deep space mission typically have long focal lengths and narrow filed of views (FOVs), and they are therefore ideal for the pole-sitter. For example, the NASA mission Galileo, launched in 1989 towards Jupiter and its satellites, was designed to perform observations of Jupiter's atmosphere composition, weather phenomena and auroras. The Solid State Imaging (SSI) instrument (29.7 kg of mass) had an 800x800 pixel sensor in the near-visible. This instrument would provide a resolution of about 27 km at nadir for the pole-sitter. The Near-Infrared Mapping Spectrometer (NIMS), instead, could provide 137-km resolution with about 18 kg of mass. Both these instruments had apertures of less than 30 cm.

Another mission, the NASA Deep Space Climate Observatory (DSCOVR), was designed for Earth observation and science from the $L_1$ Lagrange point, which is located approximately 1.5 million km from the Earth, of the same order as the distance of the pole-sitter mission (where angular size of the Earth disc is approximately 0.5 deg). Despite that this mission was initially canceled, its payload would be similar to that which could be used on a pole-sitter spacecraft. The Earth Polychromatic Imaging Spectrometer (EPIC) was designed to study ozone, aerosols, clouds, sulfur dioxide, precipitable water vapor, volcanic ash and UV irradiance. It offered a 2048x2048 pixel image in the near visible, with an aperture of 30 cm and mass of 65 kg.

At pole-sitter distance, it would offer a resolution of about 14.5 km. A complete discussion on potential applications enabled by such instrumentation is found in Ref. [2]; suffice to underline that all these instruments are well below the 100 kg mass assumed in the pole-sitter design.

Concerning the use of the pole-sitter for telecommunications, the main application would be its use as a low-bandwidth data relay with polar regions, and may be particularly useful in the southern hemisphere, where there are key Antarctic research activities ongoing and communication capabilities are limited. McInnes and Mulligan [5] envisaged possible applications including data links for scientific experiments, links to automated weather stations, emergency airfields and telemedicine. In the same work, the authors proposed the use of polar stationary spacecraft as data relay for future NOAA polar orbiting satellites, such as the NPOESS system. In this case, the telecommunication subsystem would be the main payload of the spacecraft. However, even for Earth science, there will be a need to download a relatively large volume of data from the spacecraft to the Earth real-time (high resolution imaging, for example). Considering the distance of the pole-sitter from the Earth, a high-gain steerable antenna will be required for either or both of these tasks.

Finally, a polar-sitter type platform could be used for high latitude ship tracking and telecommunications, and to support future high-latitude oil and gas exploration, especially if northern sea routes open due to climate change.[*] We refer again to Ref. [2] for further discussion on possible applications.

## V. Conclusions

In this paper a full, preliminary mission analysis and systems design of a near-term and far-term pole-sitter mission is provided, where the distinction comes from the use of either existing, solar electric propulsion (SEP) or more far-term hybrid SEP and solar sail propulsion. The platform would provide a vantage view point on either pole of the Earth, with essentially unlimited temporal resolution (real-time observations) by means of one spacecraft only. Optimal transfers from north to south and vice-versa allow observation of the pole that is lit, at no extra cost in terms of propellant consumption. Moreover, in some particular cases propellant savings can be achieved through the use of these transfers, allowing for an extension of the mission lifetime or alternatively an increase in the payload mass. Using the full potential of either a Soyuz or Ariane 5 launch vehicle, a systems mass budget demonstrated that it is potentially possible to maintain a 100-kg payload in the pole-sitter orbit for at least 4 years for the short-term SEP-only mission, and 6 years or more for the far-term hybrid mission.

[*] http://www.esa.int/esaEO/SEMT7TRTJRG_index_0.html [cited 17/08/2012].

## Acknowledgements

This work was funded by the European Research Council, as part of project 227571 VISIONSPACE. The authors thank Dr. Victor M. Becerra, of the School of Systems Engineering, University of Reading, Reading, UK for providing the software PSOPT freely, as well as advices on its use.

## References

[1] Wertz, J. R. and Larson, W. J. (eds.), *Space Mission Analysis and Design, Third Edition*, Space Technology Library, Microcosm press/Kluwer Academic Publishers, El Segundo, California, USA, 1999.

[2] Ceriotti, M., Diedrich, B. L. and McInnes, C. R., "Novel Mission Concepts for Polar Coverage: An Overview of Recent Developments and Possible Future Applications," *Acta Astronautica*, Vol. 80, 2012, pp. 89-104. doi: 10.1016/j.actaastro.2012.04.043

[3] Anderson, P. C. and Macdonald, M., "Extension of the Molniya Orbit Using Low-Thrust Propulsion," *21st AAS/AIAA Space Flight Mechanics Meeting*, AAS 11-236, AIAA, New Orleans, USA, 2011.

[4] Anderson, P. C. and Macdonald, M., "Extension of Earth Orbits Using Low-Thrust Propulsion," *61st International Astronautical Congress (IAC 2010)*, Prague, Czech Republic, 2010.

[5] McInnes, C. R. and Mulligan, P., "Final Report: Telecommunications and Earth Observations Applications for Polar Stationary Solar Sails," National Oceanographic and Atmospheric Administration (NOAA)/University of Glasgow, Department of Aerospace Engineering, 2003, www.osd.noaa.gov/rpsi/polesitter.telecommunications.pdf [retrieved 16 November 2010].

[6] Driver, J. M., "Analysis of an Arctic Polesitter," *Journal of Spacecraft and Rockets*, Vol. 17, No. 3, 1980, pp. 263-269. doi: 10.2514/3.57736

[7] McInnes, C. R., *Solar Sailing: Technology, Dynamics and Mission Applications*, Springer-Praxis Books in Astronautical Engineering, Springer-Verlag, Berlin, 1999.

[8] Mori, O., Sawada, H., Funase, R., Endo, T., Morimoto, M., Yamamoto, T., Tsuda, Y., Kawakatsu, Y. and Kawaguchi, J. i., "Development of First Solar Power Sail Demonstrator - Ikaros," *21st International Symposium on Space Flight Dynamics (ISSFD 2009)*, CNES, Toulouse, France, 2009.

[9] Johnson, L., Whorton, M., Heaton, A., Pinson, R., Laue, G. and Adams, C., "Nanosail-D: A Solar Sail Demonstration Mission," *Acta Astronautica*, Vol. 68, No. 5-6, 2011, pp. 571–575. doi: 10.1016/j.actaastro.2010.02.008

[10] Ceriotti, M. and McInnes, C. R., "Generation of Optimal Trajectories for Earth Hybrid Pole-Sitters," *Journal of Guidance, Control, and Dynamics*, Vol. 34, No. 3, 2011, pp. 847-859. doi: 10.2514/1.50935

[11] Forward, R. L., "Statite: A Spacecraft That Does Not Orbit," *Journal of Spacecraft and Rockets*, Vol. 28, No. 5, 1991, pp. 606-611.
doi: 10.2514/3.26287

[12] Waters, T. J. and McInnes, C. R., "Periodic Orbits above the Ecliptic in the Solar-Sail Restricted Three-Body Problem," *Journal of Guidance, Control, and Dynamics*, Vol. 30, No. 3, 2007, pp. 687-693.
doi: 10.2514/1.26232

[13] Leipold, M. and Götz, M., "Hybrid Photonic/Electric Propulsion," Kayser-Threde GmbH, Technical Report SOL4-TR-KTH-0001, ESA contract No. 15334/01/NL/PA, Munich, Germany, 2002, January 2002.

[14] Baig, S. and McInnes, C. R., "Artificial Three-Body Equilibria for Hybrid Low-Thrust Propulsion," *Journal of Guidance, Control, and Dynamics*, Vol. 31, No. 6, 2008, pp. 1644-1655.
doi: 10.2514/1.36125

[15] Mengali, G. and Quarta, A. A., "Trajectory Design with Hybrid Low-Thrust Propulsion System," *Journal of Guidance, Control, and Dynamics*, Vol. 30, No. 2, 2007, pp. 419-426.
doi: 10.2514/1.22433

[16] Mengali, G. and Quarta, A. A., "Tradeoff Performance of Hybrid Low-Thrust Propulsion System," *Journal of Spacecraft and Rockets*, Vol. 44, No. 6, 2007, pp. 1263-1270.
doi: 10.2514/1.30298

[17] Simo, J. and McInnes, C. R., "Displaced Periodic Orbits with Low-Thrust Propulsion," *19th AAS/AIAA Space Flight Mechanics Meeting*, AAS 09-153, American Astronautical Society, Savannah, Georgia, USA, 2009.

[18] Heiligers, J., Ceriotti, M., McInnes, C. R. and Biggs, J. D., "Displaced Geostationary Orbit Design Using Hybrid Sail Propulsion," *Journal of Guidance, Control, and Dynamics*, Vol. 34, No. 6, 2011, pp. 1852-1866.
doi: 10.2514/1.53807

[19] Lazzara, M. A., Coletti, A. and Diedrich, B. L., "The Possibilities of Polar Meteorology, Environmental Remote Sensing, Communications and Space Weather Applications from Artificial Lagrange Orbit," *Advances in Space Research*, Vol. 48, No. 11, 2011, pp. 1880-1889.
doi: 10.1016/j.asr.2011.04.026

[20] Ceriotti, M. and McInnes, C. R., "Systems Design of a Hybrid Sail Pole-Sitter," *Advances in Space Research*, Vol. 48, No. 11, 2011, pp. 1754–1762.
doi: 10.1016/j.asr.2011.02.010

[21] Heiligers, J., Ceriotti, M., McInnes, C. R. and Biggs, J. D., "Design of Optimal Earth Pole-Sitter Transfers Using Low-Thrust Propulsion," *Acta Astronautica*, Vol. 79, 2012, pp. 253–268.
doi: 10.1016/j.actaastro.2012.04.025

[22] Heiligers, J., Ceriotti, M., McInnes, C. R. and Biggs, J. D., "Design of Optimal Transfers between North and South Pole-Sitter Orbits," *22nd AAS/AIAA Space Flight Mechanics Meeting*, AIAA, Charleston, South Carolina, USA, 2012.

[23] Becerra, V. M., "Solving Complex Optimal Control Problems at No Cost with Psopt," *IEEE Multi-conference on Systems and Control*, IEEE, Yokohama, Japan, 2010, pp. 1391-1396.

[24] Wächter, A. and Biegler, L. T., "On the Implementation of a Primal-Dual Interior Point Filter Line Search Algorithm for Large-Scale Nonlinear Programming," *Mathematical Programming*, Vol. 106, No. 1, 2006, pp. 25-57.

[25] Brophy, J., "Advanced Ion Propulsion Systems for Affordable Deep-Space Missions," *Acta Astronautica*, Vol. 52, No. 2-6, 2003, pp. 309-316.
doi: 10.1016/S0094-5765(02)00170-4

[26] Leiter, H. J., Killinger, R., Bassner, H., Müller, J., Kukies, R. and Fröhlich, T., "Development and Performance of the Advanced Radio Frequency Ion Thruster Rit-Xt," *28th International Electric Propulsion Conference (IEPC 2003)*, Toulouse, France, 2003.

[27] Funase, R., Mori, O., Tsuda, Y., Shirasawa, Y., Saiki, T., Mimasu, Y. and Kawaguchi, J., "Attitude Control of Ikaros Solar Sail Spacecraft and Its Flight Results," *61st International Astronautical Congress (IAC 2010)*, IAF, Prague, Czech Republic, 2010.

[28] Dachwald, B., Mengali, G., Quarta, A. A. and Macdonald, M., "Parametric Model and Optimal Control of Solar Sails with Optical Degradation," *Journal of Guidance, Control, and Dynamics*, Vol. 29, No. 5, 2006, pp. 1170-1178.
doi: 10.2514/1.20313

[29] Kawaguchi, J. i., Mimasu, Y., Mori, O., Funase, R., Yamamoto, T. and Tsuda, Y., "Ikaros - Ready for Lift-Off as the World's First Solar Sail Demonstration in Interplanetary Space," *60th International Astronautical Congress (IAC 2009)*, IAC-09-D1.1.3, International Astronautical Federation, Daejeon, Korea, 2009.

[30] Murphy, D. M., Murphey, T. W. and Gierow, P. A., "Scalable Solar-Sail Subsystem Design Concept," *Journal of Spacecraft and Rockets*, Vol. 40, No. 4, 2003, pp. 539-547.
doi: 10.2514/2.3975